PNNL-23893

Pacific Northwest
NATIONAL LABORATORY
Proudly Operated by Battelle Since 1965

# Active Time-Domain Reflectometry for Tamper Indication in Unattended Monitoring Systems for Safeguards

## December 2014

JR Tedeschi
LE Smith
DE Moore
DM Sheen
RC Conrad

U.S. DEPARTMENT OF
ENERGY

Prepared for the U.S. Department of Energy
under Contract DE-AC05-76RL01830

PACIFIC NORTHWEST NATIONAL LABORATORY
*operated by*
BATTELLE
*for the*
UNITED STATES DEPARTMENT OF ENERGY
*under Contract DE-AC05-76RL01830*

**Printed in the United States of America**

**Available to DOE and DOE contractors from the**
**Office of Scientific and Technical Information,**
**P.O. Box 62, Oak Ridge, TN 37831-0062;**
**ph: (865) 576-8401**
**fax: (865) 576-5728**
**email: reports@adonis.osti.gov**

**Available to the public from the National Technical Information Service,**
**U.S. Department of Commerce, 5285 Port Royal Rd., Springfield, VA 22161**
**ph: (800) 553-6847**
**fax: (703) 605-6900**
**email: orders@ntis.fedworld.gov**
**online ordering: http://www.ntis.gov/ordering.htm**

PNNL-23893

# Time-Domain Reflectometry for Tamper Indication in Unattended Monitoring Systems for Safeguards

JR Tedeschi
LE Smith
DE Moore
DM Sheen
RC Conrad

December 2014

Prepared for
the U.S. Department of Energy
under Contract DE-AC05-76RL01830

Pacific Northwest National Laboratory
Richland, Washington  99352

# Abstract

The International Atomic Energy Agency (IAEA) continues to expand its use of unattended, remotely monitored measurement systems. An increasing number of systems and an expanding family of instruments create challenges in terms of deployment efficiency and the implementation of data authentication measures. Pacific Northwest National Laboratory (PNNL) leads a collaboration that is exploring various tamper-indicating (TI) measures that could help to address some of the long-standing detector and data-transmission authentication challenges with IAEA's unattended systems. PNNL is investigating the viability of active time-domain reflectometry (TDR) along two parallel but interconnected paths: (1) swept-frequency TDR as the highly flexible, laboratory gold standard to which field-deployable options can be compared, and (2) a low-cost commercially available spread-spectrum TDR technology as one option for field implementation. This report describes PNNL's progress and preliminary findings from the first year of the study, and describes the path forward.

# Acknowledgments

This research was supported by the U.S. National Nuclear Security Administration (NNSA) Office of Nonproliferation and International Security (NA-24), and its Next Generation Safeguards Initiative, under Contract DE-AC05-76RL01830 with the U.S. Department of Energy.  Pacific Northwest National Laboratory is a multi-program national laboratory operated by Battelle for the U.S. Department of Energy.

The authors would like to thank Cesare Liguori, Thierry Pochet, and Roman Simlinger of the IAEA for their helpful insights and collaboration.

# Acronyms and Abbreviations

| | |
|---|---|
| ASIC | application specific integrated circuit |
| BPSK | binary phase shift keyed |
| DSSS | direct sequence spread spectrum |
| DUT | device under test |
| EMI | electromagnetic interference |
| FEE | front-end electronics |
| HPF | high pass filter |
| IAEA | International Atomic Energy Agency |
| INL | Idaho National Laboratory |
| LANL | Los Alamos National Laboratory |
| LPF | low pass filter |
| NGSI | Next Generation Safeguards Initiative |
| PCB | custom printed circuit board |
| PNNL | Pacific Northwest National Laboratory |
| PTFE | polytetrafluoroethylene |
| SMA | sub-miniature version A |
| SSTDR | spread spectrum time domain reflectometry |
| TDR | time domain reflectometry |
| TI | tamper-indicating |
| UMS | unattended monitoring system |
| VNA | vector network analyzer |

# Contents

# Figures

# Tables

# 1.0 Introduction

Remotely monitored, unattended nondestructive assay systems are central to the International Atomic Energy Agency's (IAEA's) ability to safeguard an expanding global fuel cycle with limited manpower and financial resources. As the number of unattended monitoring instruments increases, the IAEA is challenged to become more efficient in the implementation of those systems, and to ensure the authenticity of data coming from an expanding family of instruments. Ensuring that the detector signals received at the IAEA cabinet are authentic is central to the independence of IAEA's safeguards conclusions. Unfortunately, traditional data security measures, for example tamper-indicating (TI) conduit, are impractical for the long separation distances (often 100 m or more) between unattended monitoring system (UMS) components. Challenges include the fact that such conduit requires detailed physical inspection by the IAEA during on-site visits, and often, the cabling is routed through multiple penetrations in difficult-to-access parts of the facility. These inspections are tedious, time-consuming, and only periodic, rather than continuous. Advanced TI options are needed, and the *IAEA Department of Safeguards Long-Term R&D Plan, 2012-2023* identifies this need for the "ability to communicate secure, authentic information…between the IAEA…and equipment in the field" (IAEA 2013).

Under support from the U.S. National Nuclear Security Administration's Next Generation Safeguards Initiative (NGSI), a multi-organization collaboration of Pacific Northwest National Laboratory (PNNL) (lead), Idaho National Laboratory (INL), and Los Alamos National Laboratory (LANL) is studying candidate TI methods for IAEA's unattended monitoring systems as part of a project known as the front-end electronics package for unattended instrumentation (FEUM). The collaborators are performing independent investigations of different candidate TI approaches: active time-domain reflectometry (PNNL), passive noise analysis (INL), and pulse-by-pulse analysis and correction of signal integrity (LANL). Among the development questions to be addressed in the project are:

- How do the fundamental characteristics of these TI candidate methods differ?
- Can TI signals be distinct and separable from the frequency spectra of common UMS sensor types?
- How effectively can the candidate methods detect common tampering scenarios?
- Are there obvious vulnerabilities in the methods and, if so, how might they be addressed?
- For promising TI methods, what are the implementation options? How might they interface with common IAEA data acquisition systems?

The project team developed two use cases, representative of IAEA UMS deployments today and the in the future, to guide the study:

1. *Use Case 1:* Retrofit of advanced TI methods into existing deployments where the sensor is co-located with the front-end electronics (FEE) (Figure 1). This is the highest priority use case because it is how the vast majority of IAEA systems are deployed today.
2. *Use Case 2:* Integration of advanced TI methods in deployments where the FEE is separated from the sensor, creating two distinct sections of cabling, one between the sensor and the FEE, and the other between the FEE and the IAEA cabinet (Figure 2).

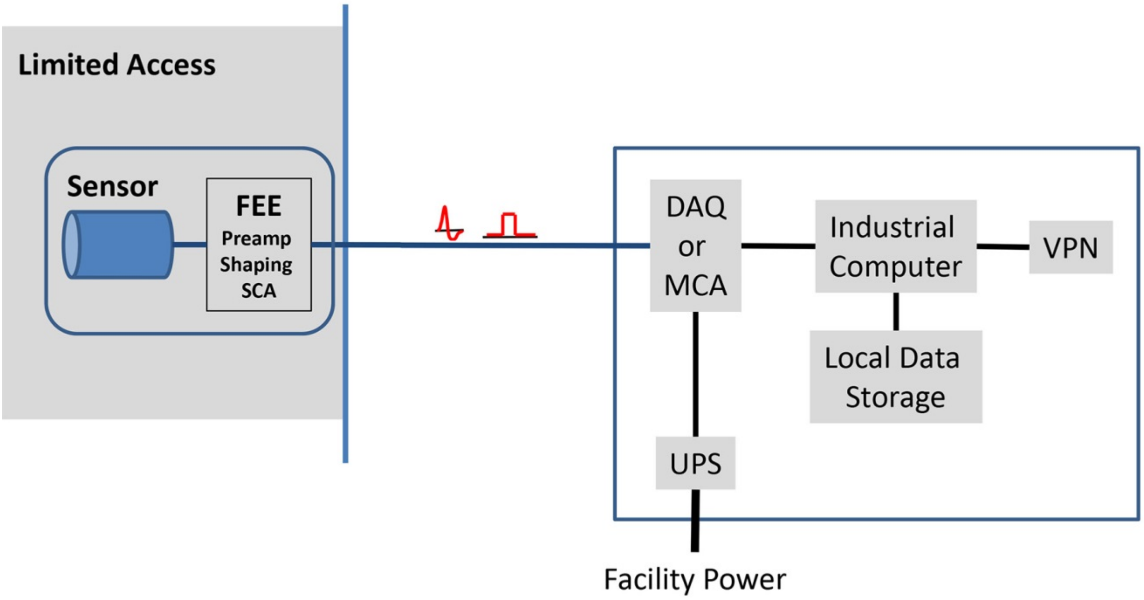

**Figure 1**. Use Case 1 in which FEEs are Co-located with the Sensors, Often Inside an Area of Limited Personnel Access

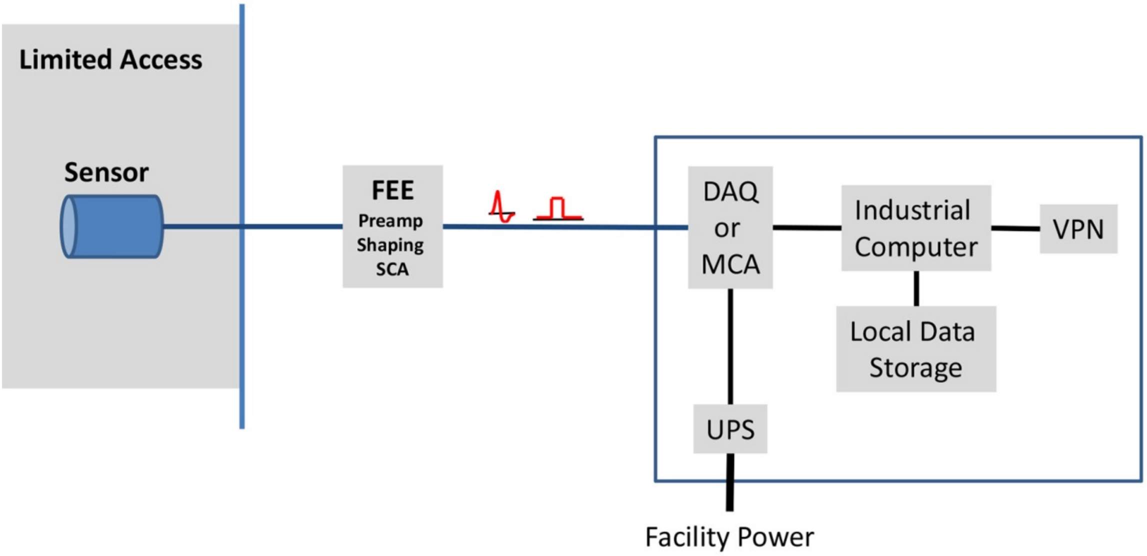

**Figure 2**. Use Case 2 in which the FEEs are Separated from the Sensor and the Cabinet

It is assumed in this study that the baseline, unperturbed condition of the cabling is verified and known upon initial installation of the UMS cabling and equipment so that TI methods for physical intrusion are focused on detecting *changes* in the cabling characteristics from that baseline. Note that while these use cases are illustrated above with a single sensor and FEE, typical IAEA deployments involve multiple sensors and multiple cables.

The NGSI study is framed by two distinct but connected tampering scenarios: (1) physical intrusion into the cabling, and (2) signal tampering (e.g., the injection of synthetic signals that emulate real signals under normal operational conditions). For either tampering scenario, the TI method should raise a flag to indicate that the instrumentation system may have been compromised and, therefore, that safeguards data produced by that instrument from that time forward may be suspect.

To date, the IAEA has not issued formal requirements for new technologies intending to address these two TI challenges. To guide the NGSI study of candidate TI methods, the project team has developed preliminary functional requirements and performance targets for the first scenario: physical intrusion into cabling (Smith et al. 2014). Cable tampering scenarios defined by the NGSI team include taps, splices, disconnects, and replacements. Metrics for evaluation of the candidate TI methods include detection probability and false-alarm rate under various operational conditions, ability to localize the tampering event, and the value of diagnostics provided by each method that could aid the IAEA in determining the likely cause of the tamper indication.

PNNL's initial investigation of the viability of active time-domain reflectometry (TDR) for the detection of physical intrusion into cabling is taking two parallel but interconnected paths: (1) swept-frequency TDR as the highly flexible, laboratory gold standard to which field-deployable options can be compared, and (2) a low-cost commercially available spread-spectrum TDR technology as one option for field implementation. This report describes PNNL's progress and preliminary findings from the first year of the study where the focus has been on building a laboratory testing and evaluation capability and performing preliminary investigations into the ability of candidate TDR methods to detect the cable tampering scenarios identified in Smith et al. (2014). Tentative PNN-L plans for the second year of the study are also provided.

## 2.0 Swept-Frequency Time-Domain Reflectometry

The swept frequency TDR measurement method is put to practice in this study using an Agilent Technologies vector network analyzer (VNA). The VNA TDR uses Fourier analysis of swept frequency domain signals, velocity of signal propagation, and transmission line impedance changes to determine both amplitude and position in time/space of reflected signals. For a standard coaxial transmission line, the line impedance is expected to be nominally continuous throughout the cable; however, if the cable now connects to a device under test (DUT), there will be a reflection if the DUT impedance does not perfectly match the impedance of the coaxial line. The reflection coefficient is defined as follows:

$$\rho = \frac{Z_{DUT} - Z_0}{Z_{DUT} + Z_0},$$

where $Z_0$ is the transmission line impedance and $Z_{DUT}$ is the impedance of the DUT. Performing an electronic calibration on the VNA (Keysight Technologies 2014) corrects for the insertion loss, impedance, and phase associated with VNA and its test cables that connect the VNA to the DUT. Therefore, this allows the VNA to perform fully calibrated amplitude and phase frequency measurements that are in response to the DUT. The VNA then performs a swept frequency domain reflection measurement and mathematically computes a time domain transform using the chirp-Z Fast Fourier Transform technique (Agilent 2012). The reflection or S11 measurement refers to the measured signal amplitude and phase received at Port 1 relative to the transmitted amplitude and phase from Port 1. The time domain data is then converted into the spatial domain by a second translation using signal phase velocity, also expressed as the velocity of light in the medium. The phase velocity for non-magnetic materials is determined using the equation shown below (Wadell ),

$$v_P = \frac{c}{\sqrt{\varepsilon_r}}$$

where c is the speed of light ($3\times10^8$ m/s), and $\varepsilon_r$ is the real part of the dielectric constant of the propagation medium. For reference, the phase velocity of in polyethylene and polytetrafluoroethylene (PTFE), are 66% and 69% of the phase velocity in free space respectively.

## 2.1 Swept Frequency TDR: Testing Arrangement

The swept frequency TDR measurements performed to date assumed Use Case 1, described previously, where the sensor and pre-amplification circuit installed in an area with limited access and the data acquisition and other circuitry/power supplies are installed within a tamper-indication housing some distance away. This leaves the cabling between those locations vulnerable for tampering, because such cabling is often not protected with TI conduit in IAEA deployments.

The block diagram of a proposed swept-frequency TDR configuration for tamper detection is shown Figure 3. The proposed configuration utilizes a diplexer, which is a 3-port device that has a common, low pass filter (LPF) and a high pass filter (HPF) port. The common-to-LPF port interface should allow the sensor signals to pass unaltered from the sensor to the DAQ; that is, the TDR signals should not perturb the sensor signal. The HPF-to-common port will allow the VNA to perform S11 measurements from the VNA to the sensor electronics location, over the full length of the exposed cable. Although in practice the sensor electronics will present a specific impedance at the end of the cable, the preliminary studies presented here included only the cable under test and various terminators that allowed flexibility in the impedance presented to the VNA.

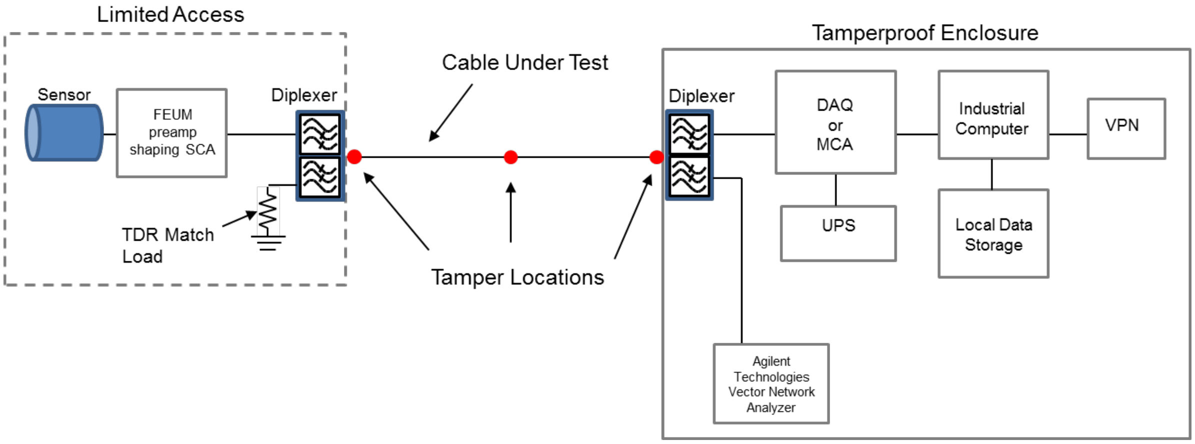

**Figure 3**. Block Diagram of Swept-Frequency TDR Implementation Concept, Assuming Use Case 1

## 2.2 Cable Tamper: Preliminary Findings

A proof-of-concept measurement was performed using the VNA to send calibrated swept-frequency signals from 50–3000 MHz into an RG174 50-ohm cable that is nominally 9.5 m long. Figure 4 displays the test arrangement showing the VNA port 1 connected to cable end 1, and cable end 2 connected to a 50-ohm termination.

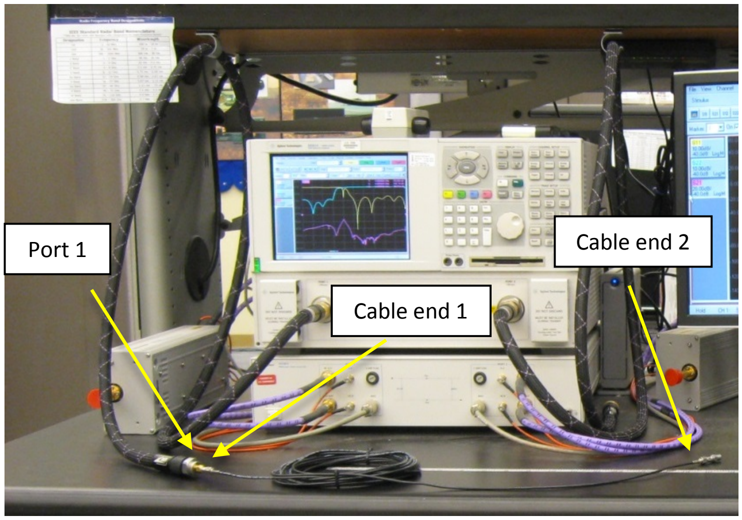

**Figure 4**. Agilent VNA with Cable under Test Connected to Port 1

A baseline reflection measurement was collected on the test cable, consistent with the assumptions in Smith et al. (2014) and to enable the monitoring of relative reflection changes due to cable tampering. At 25 cm from the end of the cable, a small section of the outer conductor on the coaxial line was cut and peeled back to allow a high-impedance probe access to the center conductor on the line. The cut in the outer conductor was approximately 1 mm × 2 mm (Figure 5). Note that in order to verify the legitimacy of the tamper, as a separate test from the VNA measurement, a function generator was connected to the cable and used to inject a 1-MHz sine wave into the cable. It was confirmed, by pushing the high-frequency probe onto the center conductor of the cable and pinching the outer conductor of the cable with the ground reference, that the sine wave could be measured on an oscilloscope.

Using the chirp-Z Fast Fourier Transform of the swept frequency domain measurement allows analysis of the response in the time domain; using the phase velocity in the medium, the location of the reflection can be determined.

Figure 5 shows the cable tamper and the reflected signal response in the spatial domain. The overlay of the baseline vs. tampered cable reveals a large reflection at 9.296 m. One can observe that even without the probe touching the center conductor, the break in the outer conductor causes an impedance change significant enough to produce a reflected signal that is 20 dB higher than the original structure of the cable; whereas, when the probe makes contact with the center conductor, the reflected signal is 40 dB higher than the original cable structure. The end of the cable is shown as the final peak above −60 dB in the baseline curve; this corresponds to 9.542 m. The measured distance from the end of the cable to the tamper location is 25.0 cm. This known tamper location can be compared to a TDR-measured distance of 24.6 cm from the cable end. This preliminary result is encouraging in terms of TDR's ability to detect cable taps, and provides an early indicator of localization accuracy and precision for such a method.

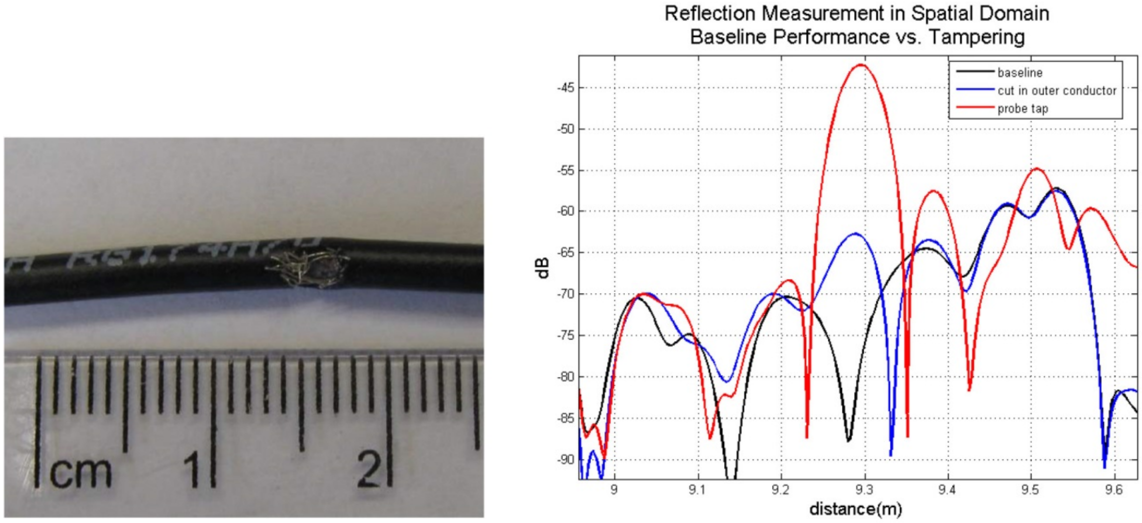

**Figure 5**. RG174 Cable Tamper and Resulting Reflection Measurements in the Spatial Domain

## 2.3 Cable Splice: Preliminary Findings

Another of the cable-tampering scenarios to be considered in the NGSI study is a cable splice, where the load of the splice is variable from open to short. As a preliminary investigation into this scenario, PNNL performed reflection measurements for a 50-m RG174 cable (shown in Figure 6) with different devices/loads at the end of the cable. Again, a baseline TDR scan was performed using a 50-ohm termination, under the assumption of good impedance matching between the transmission cable and the sensor electronics package. (Note that this assumption is not always valid in IAEA UMS deployments and the effects of suboptimal impedance matching in the baseline scan will need further investigation.) Figure 7 shows the multiple loads that were connected to the end of the cable for these early characterization experiments. Note that similar measurements performed with a segmented 93 ohm RG71 cable and are discussed in Appendix A.

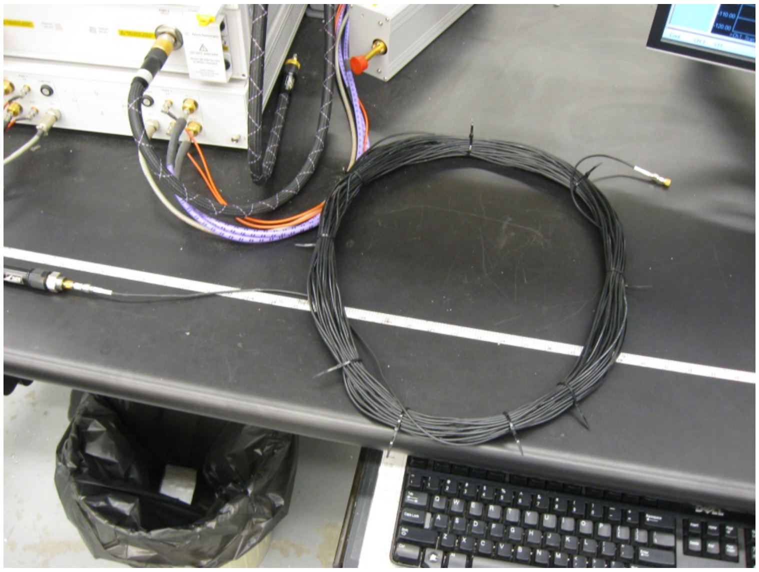

**Figure 6**. 50-m RG174 Cable under Test Connected to VNA

**Figure 7**. Devices under Test (DUT) Used for Reflection Measurements at End of 50-m long RG174 Cable

The S11 reflection-based measurements are displayed in Figure 8 in the spatial domain applying the velocity factor in RG174 of 0.66 (LiveWire 2014). Table 1 lists the relative reflected signal amplitude compared to the baseline of a 50-ohm termination. The measurement results below indicate that under laboratory conditions where electromagnetic interference (EMI) is kept to a minimum; the current swept-frequency TDR configuration is capable of detecting all but the 20-dB attenuator/pad case, assuming effective monitoring and analysis algorithms.

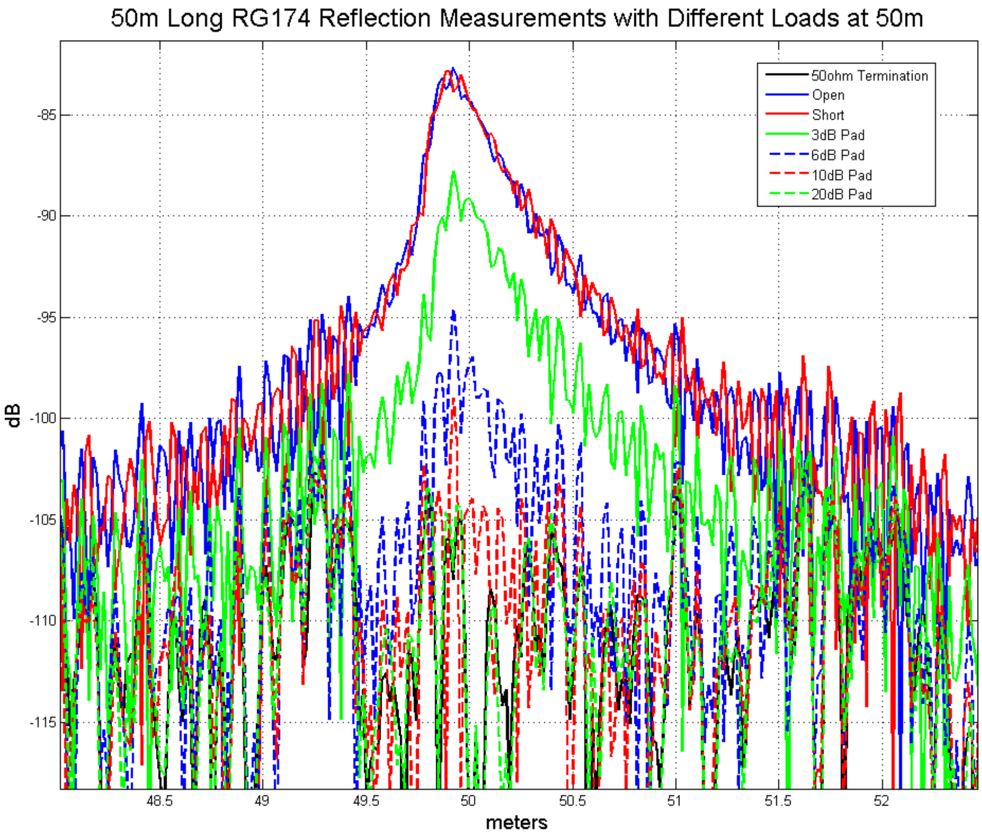

**Figure 8**. Reflection Measurement Results for Different Loads at 50 m on RG174

**Table 1**. Measurement Delta between Different Loads and 50-ohm Termination at 50 m on RG174 Cable

| Load | S11 Response (dB) | Delta from Perfect Match (dB) |
|---|---|---|
| 50 ohm | −108 | 0 |
| Open | −82.66 | 25.34 |
| Short | −83.86 | 24.14 |
| 3 dB Pad | −87.76 | 20.24 |
| 6 dB Pad | −94.52 | 13.48 |
| 10 dB Pad | −98.98 | 9.02 |
| 20 dB Pad | −107.5 | 0.5 |

A second variant of the splice scenario was explored, in which the splicing connector introduces a significant difference in the length of the cable being monitored. For this experiment, the Narda Microwave coupler shown in Figure 9 was installed at the end of the same 50 m RG174 cable described above. The coupler has a specified operating bandwidth of 0.5–18 GHz and the insertion loss to the coupled port of 20 dB.

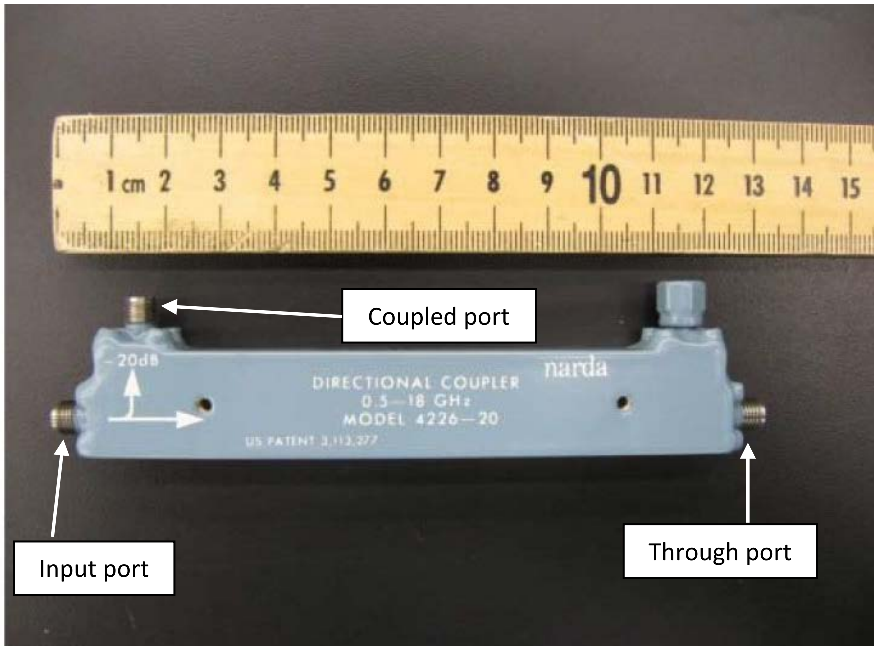

**Figure 9**. Narda Microwave Coupler

A baseline scan, without the device, was compared to a scan with the device installed with different termination values. It was observed that impedance changes on the −20 dB coupled port produced no noticeable changes in the magnitude of the reflection measurements; however, it may be that directional couplers with a lesser degree of coupling and reduced isolation could produce noticeable reflections due to impedance changes on the coupled port; as the insertion loss from the input port to the coupled port will be reduced, the reflected signal amplitude from the coupled port will be stronger, and will provide added dynamic range above the thermal noise background.

Figure 10 compares three measurement results on the 50 m RG174 cable: (1) the baseline response that is the 50-m cable with a 50-ohm termination, (2) the coupler installed at the end of the 50-m cable with a 50-ohm termination installed on the through port of the coupler, and (3) the coupler installed at the end of the 50-m cable with an open on the through port.

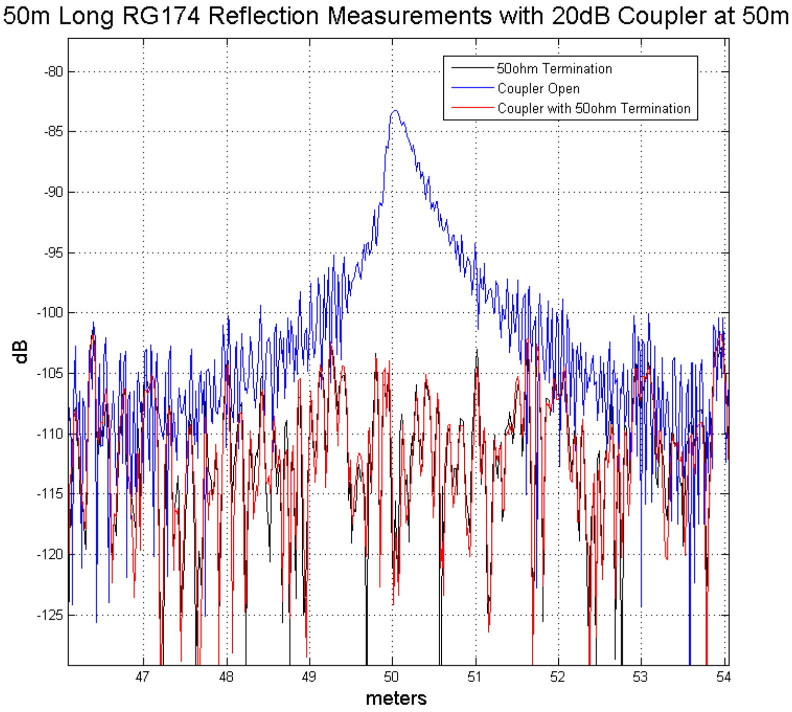

**Figure 10**. Narda Coupler Reflection Measurements

The measurement results show that because the coupler itself is very well-matched (by design) to the cable impedance, no significant change in the magnitude of the reflected signal features is evident, for the case of 50-ohm termination on the output of the couplers through line port. The response from the open load at the through line of the coupler shows a large amplitude difference, similar to the reflection response to the open at the cable end in Figure 9. Because the coupler introduces added electrical length to the cable, this can be further investigated by comparing the response in time/space of the open at the end of the cable to the open at the through line of the coupler. Figure 11 reveals a spatial shift of 13 cm, a distance consistent with the physical length of the Narda Microwave coupler. This proof-of-concept experiment indicates that the time/spatial location of known reflections in an un-tampered cable could be used to detect cable splices that introduce only small changes in the length of the signal transmission path. It remains to be investigated whether the relative location of the reflections for a well-terminated cable can also reveal small changes in path length.

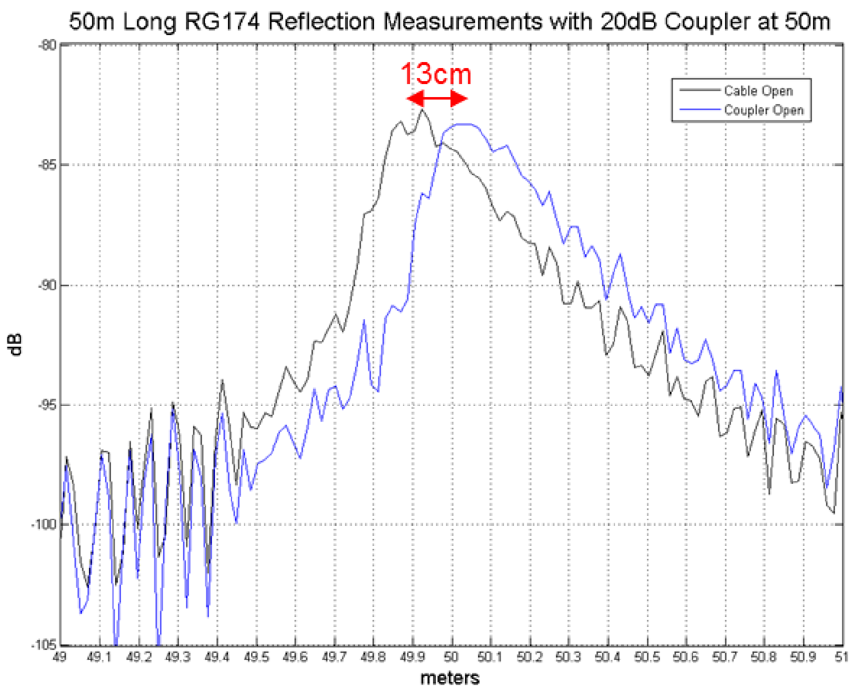

**Figure 11**. Cable Open vs. Coupler Open Spatial Shift

# 3.0 Spread-Spectrum TDR with LiveWire

LiveWire [from LiveWire Innovation (LiveWire 2014)] was designed to operate continually in the background of a system to monitor for cable breaks and shorts without influencing the operation of the system being monitoring. LiveWire uses a spread spectrum TDR (SSTDR) technique with low-power signals that, when viewed in the frequency domain, appear as noise rather than continuous wave or swept continuous wave signals. For SSTDR to generate its ‘noise’ frequency, a sine wave that has been shaped into a square wave is multiplied by a pseudo noise correlator; this generates a direct sequence spread spectrum (DSSS) binary phase shift keyed (BPSK) signal (Smith et al. 2005). This DSSS BPSK signal is then mixed with the original sine wave to produce a spread-frequency spectrum signal that is injected into the cable. The return signal, after reflection from discontinuities in the transmission path, includes any added noise or other frequency content from the system being monitored. The reference signal is the original sine wave with a variable phase delay applied; adjusting the phase delay allows for localization of the discontinuities in the cable. The reflected signal is cross-correlated with a reference signal to determine the location of the discontinuity.

LiveWire implements their SSTDR method in a number of form factors but in this study, the primary focus is a small, low power, portable application specific integrated circuit (ASIC). The design of the ASIC is tailored to the detection of faults, either open or shorts, on power or communication networks without causing any disturbances of its own. A primary user of the device to date has been the aircraft industry. This stand-alone package can be customized for specific uses, and is the device that has been of interest to the IAEA.

In 2010, the IAEA began an investigation of the LiveWire TDR method for applicability in both surveillance and unattended radiation detection systems. The very early proof-of-concept tests performed by the IAEA and a LiveWire representative were inconclusive but encouraging. IAEA continued its study of LiveWire with a focus on surveillance applications using analog cameras (e.g., radiation-hardened cameras). IAEA staff purchased a LiveWire ASIC, designed and fabricated printed circuit boards (PCBs) to support the ASIC and the accompanying microcontroller, and developed a software interface to support testing. By 2013, those tests were sufficiently successful to support a dedicated integration effort for IAEA surveillance needs. A project under the German Support Program to the IAEA is now underway to integrate the LiveWire ASIC in the controller module for one of the IAEA analog camera systems.(a)

While the IAEA's study of LiveWire for surveillance has proceeded significantly in recent years, there has been no corresponding progress on its viability for unattended radiation detection systems. PNNL, in the course of its TDR investigation in the NGSI project, is positioned to inform the IAEA on this topic. In recognition of this opportunity, IAEA provided (in October 2014) sample implementations of its PCBs, microcontroller, and software to PNNL as the start of a collaborative investigation on LiveWire for IAEA UMS.

## 3.1 LiveWire: Testing Arrangement

Prior to receipt of IAEA's LiveWire components and information, PNNL purchased three of the LiveWire ASICs and developed a breadboard platform to support the interface between the ASIC and microcontroller. PNNL selected the Arduino DUE microcontroller, rather than the Atmega644A used by the IAEA. The Arduino DUE, with its 84-MHz 32-bit microcontroller, is able to take advantage of the 48-MHz serial peripheral interface offered by the LiveWire ASIC for more efficient data capture, when compared to the ATmega644A (20-MHz 8-bit microcontroller). Also, Arduino boards include additional components that facilitate efficient programming and maintainability; for example, a standard hardware interface, native USB-serial communication, and a significant archive of related code from the open source community. The latter is particularly important, given the IAEA's recent and ongoing emphasis on software sustainability, particularly in support of technologies that spawn from Member State R&D programs like NGSI.

PNNL staff worked with LiveWire documentation and technical support to understand the command set and format for communications with the ASIC, and the Arduino DUE was programmed accordingly. The ASIC was configured and connected to the Arduino DUE (Figure 12) using an appropriate filter network on the breadboard. PNNL has adopted, at least preliminarily, the IAEA's circuit diagrams for the ASIC filter network, which matched the filter network recommended by LiveWire in their documentation. More investigation is needed as to the filter networks utilized with the LiveWire ASIC, particularly as it pertains to the cabling typically used in IAEA UMS deployments.

PNNL has also exercised the IAEA's graphical user interface for communication with the ASIC and the display of output from the device; a screen shot from that software is shown in Figure 13 and indicates that a number of variable parameters can be controlled through it.

---

(a) Roman Simmlinger, International Atomic Energy Agency, personal communication, 2014.

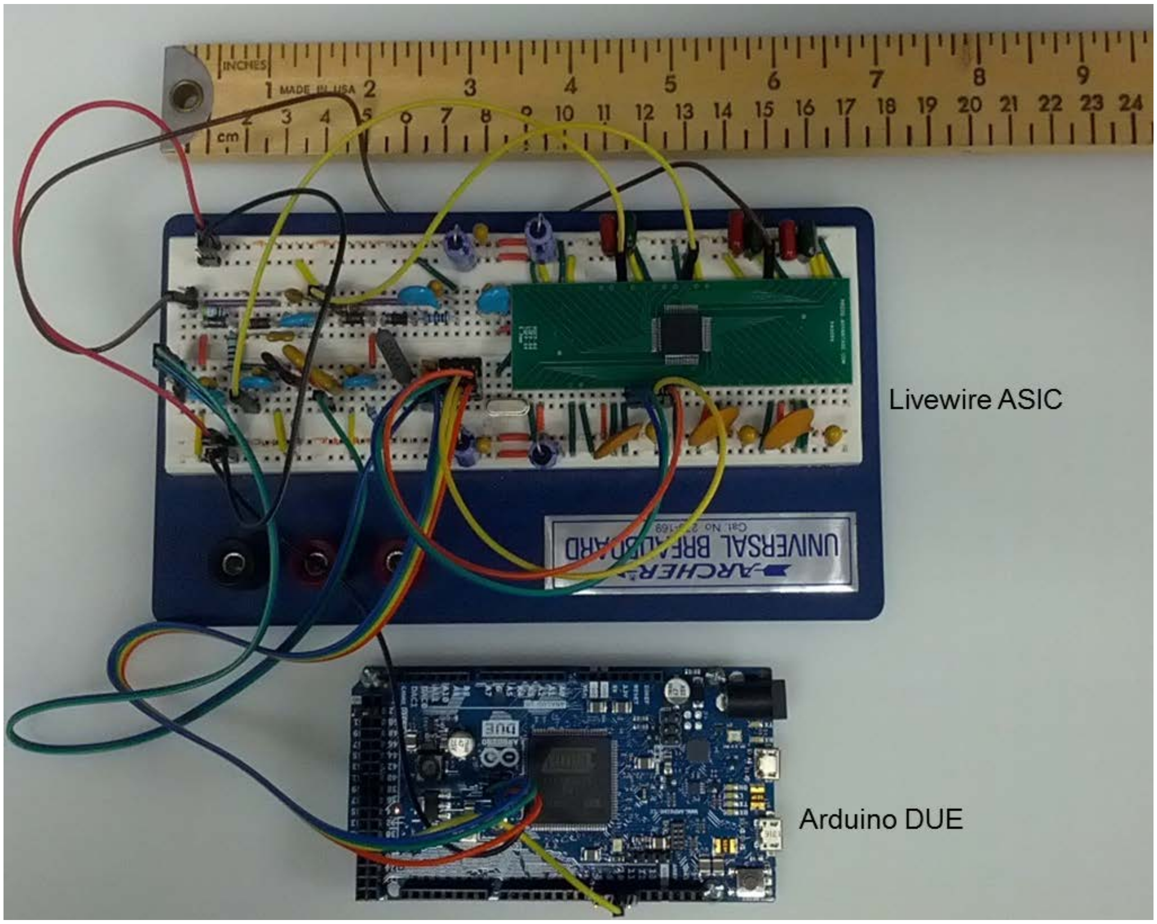

**Figure 12**. LiveWire ASIC Breadboard Circuit Connected to Arduino Controller

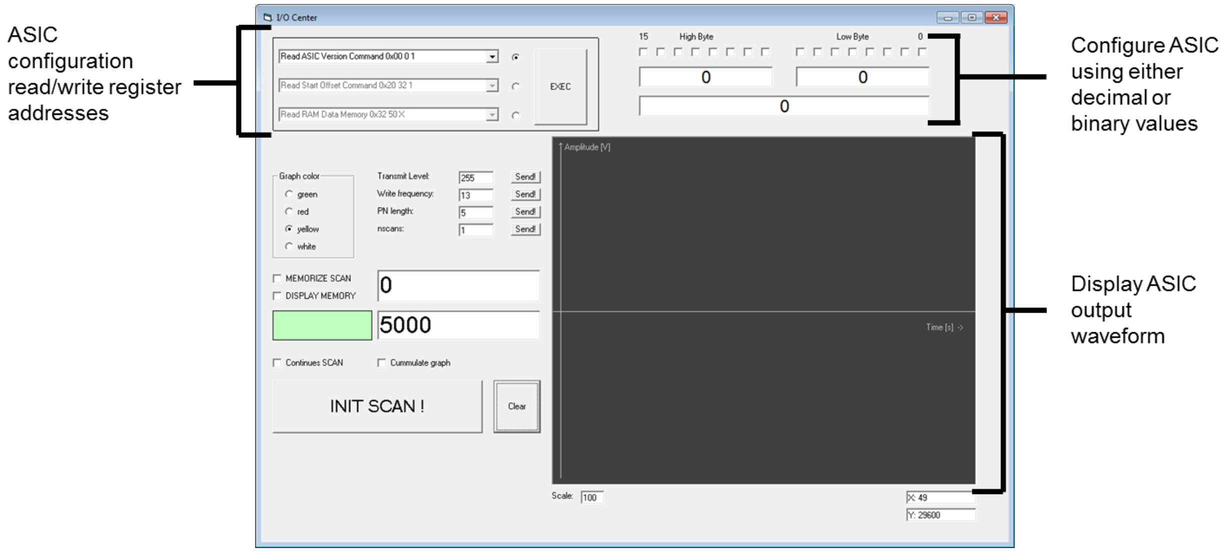
ASIC configuration read/write register addresses

Configure ASIC using either decimal or binary values

Display ASIC output waveform

I/O Center

● Read ASIC Version Command 0x00 0 1
○ Read Start Offset Command 0x20 32 1
○ Read RAM Data Memory 0x32 50 X

15 High Byte ☐ ☐ ☐ ☐ ☐ ☐ ☐ ☐ Low Byte ☐ ☐ ☐ ☐ ☐ ☐ ☐ ☐ 0

High Byte: 0
Low Byte: 0
0

Graph color
○ green
○ red
● yellow
○ white

Transmit Level: 255
Write frequency: 13
PN length: 5
nscans: 1

☐ MEMORIZE SCAN
☐ DISPLAY MEMORY

0

5000

☐ Continues SCAN
☐ Cummulate graph

Scale: 100
X: 49
Y: 29600

**Figure 13**. LiveWire ASIC Graphical User Interface

## 3.2 LiveWire: Preliminary Findings

PNNL staff familiarized themselves with the LiveWire ASIC input and output through a series of very simple functional tests, using the same representative cabling setup used in the swept-spectrum TDR work described earlier: 50-meter RG174 cable terminated with varying termination at the end, the LiveWire scan frequency was set to 24 MHz, and 250 scans averaged before displaying the output through the user interface panel. Figures 14 and 15 show the time-domain response for 50-ohm termination and open circuit, respectively. The results are as expected, where the reflection from the end of a properly terminated cable is negligible, while the open-circuit produces a large reflected signal well-separated in time from the large reflection that occurs at very early times (presumably from an impedance mismatch near the injection point of the signal into the cable). More investigation is needed to ensure proper coupling between the ASIC output and the cabling typical of IAEA UMS deployments and to more fully understand the transmitted and reflected signals. This investigation will inform, for example, PNNL's modification of the PCB to support the monitoring of cabling for radiation detection instrumentation. Initial conversations between PNNL and LiveWire engineers indicate that the standard filter network originally recommended by LiveWire (and used in the IAEA's implementation) is designed for 110-ohm transmission lines, whereas most cabling for IAEA UMS is either 50 or 75 ohm. It remains to be determined if LiveWire can achieve better performance via impedance matching the filter network to the cable under test for better energy transfer, and if the impedance matching of the filter network to the cable under test will make the sensors performance more susceptible to being influenced by LiveWire.

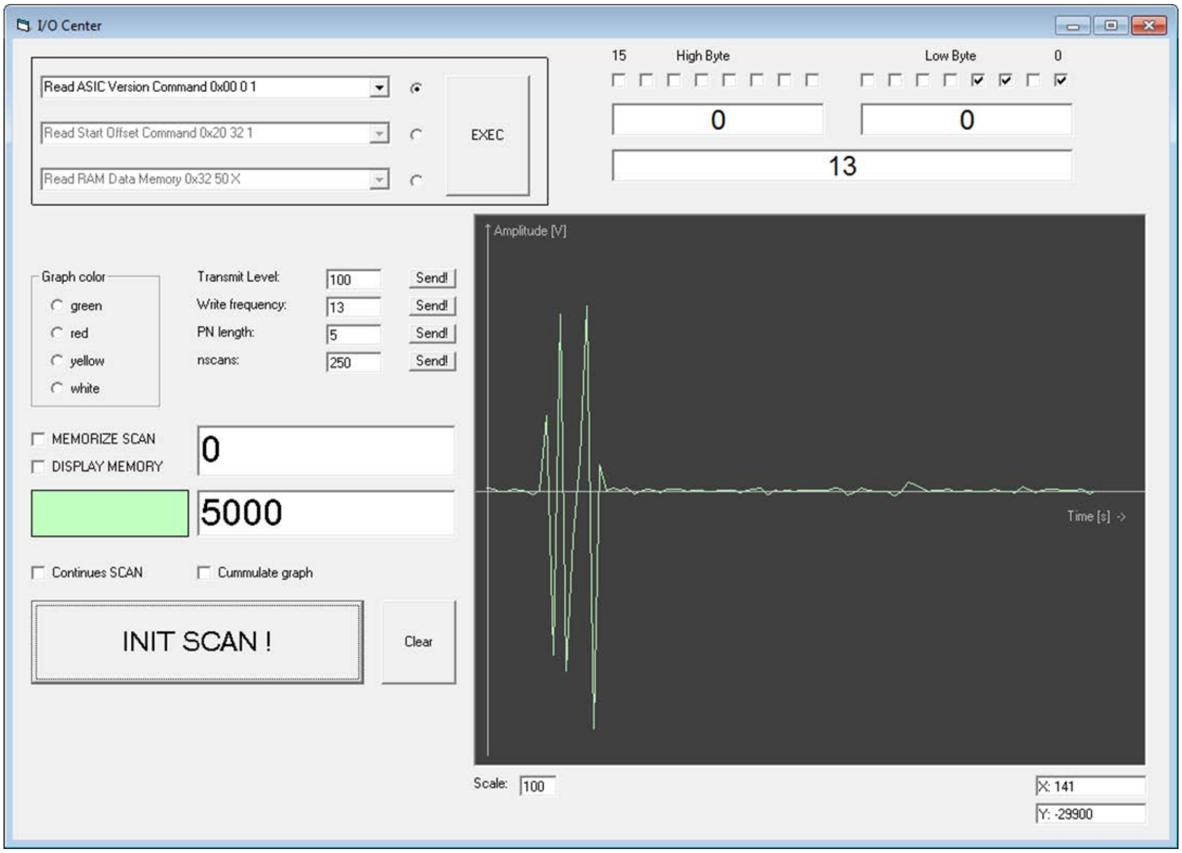

● Read ASIC Version Command 0x00 0 1
○ Read Start Offset Command 0x20 32 1
○ Read RAM Data Memory 0x32 50 X

☐ ☐ ☐ ☐ ☐ ☐ ☐ ☐ ☐ ☐ ☐ ☐ ☑ ☑ ☐ ☑

0
0
13

○ green
○ red
○ yellow
○ white

Transmit Level: 100
Write frequency: 13
PN length: 5
nscans: 250

☐ MEMORIZE SCAN
☐ DISPLAY MEMORY

0
5000

☐ Continues SCAN
☐ Cummulate graph

Scale: 100
X: 141
Y: -29900

**Figure 14**. LiveWire Response with 50-m RG174 Cable with 50-ohm Termination at Cable End

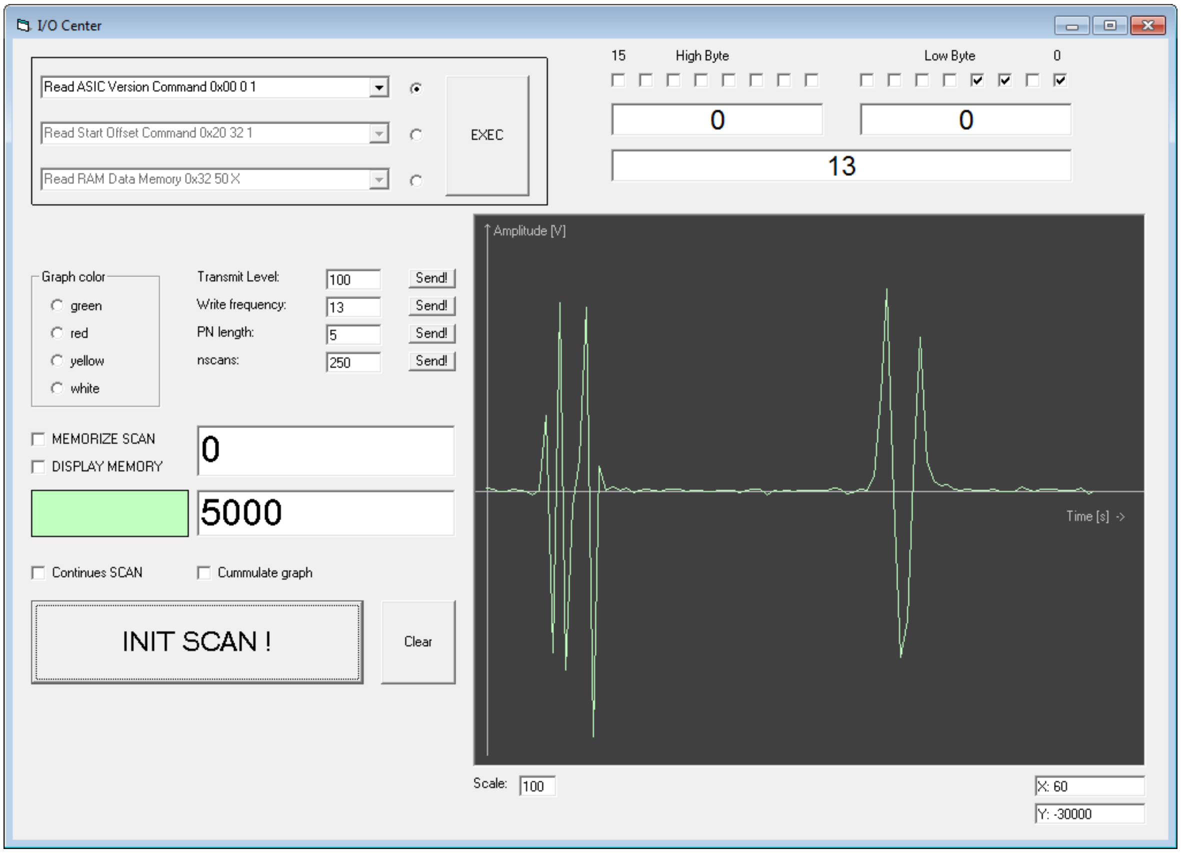

● Read ASIC Version Command 0x00 0 1
○ Read Start Offset Command 0x20 32 1
○ Read RAM Data Memory 0x32 50 X

☐ ☐ ☐ ☐ ☐ ☐ ☐ ☐ ☐ ☐ ☐ ☐ ☑ ☑ ☐ ☑

0
0
13

Transmit Level: 100
Write frequency: 13
PN length: 5
nscans: 250

☐ MEMORIZE SCAN
☐ DISPLAY MEMORY
0
5000
☐ Continues SCAN
☐ Cummulate graph

Scale: 100
X: 60
Y: -30000

**Figure 15**. LiveWire Response to 50-m Cable with Open Circuit at Cable End

## 4.0 Conclusions and Next Steps

PNNL has successfully developed a laboratory testing capability for the evaluation of candidate TDR methods, for IAEA's unattended monitoring applications. A versatile, fully calibrated, ultra-wideband (10 MHz to 67 GHz) swept-frequency TDR bench top instrument will be the high-performance baseline against which the commercially available LiveWire technology, which has a significantly more restrictive range of operation, will be evaluated. Proof-of-principle measurements using both TDR methods have been completed and have set the stage for a more thorough comparative evaluation using the cable tampering scenarios and evaluation metrics defined previously by the NGSI project team.

More specifically, FY15 tasking will compare the two systems' performance for (1) detecting impedance changes/line taps in 0–50 m long cables, (2) vulnerability to noise environments, (3) vulnerability to EMI, (4) localization accuracy, and (5) performance when installed in line with radiation detection sensors and pulse-processing electronics, in configurations representative of IAEA UMS deployments.

In order to complete this comparative evaluation, a number of preparatory tasks must be completed:

- Modify PCB design for support of the LiveWire ASIC to be compatible with radiation detection systems and the Arduino microcontroller.
- Develop basic data acquisition and visualization tools for LiveWire that will allow a more complete exploration of the input parameter space (e.g., input frequency), and the effect on the output. The use of proprietary and custom software will be minimized to the extent possible, toward the goal of software sustainability in the future.
- Develop data analysis and "alarming" algorithms for both swept-frequency TDR and LiveWire data, to support quantitative studies of efficacy that acknowledge the tradeoff between the probability of detecting tampering events and false-alarm rates.

PNNL will continue to share lessons learned with LANL and INL as they continue their investigations of other candidate tamper-indication methods.

# 5.0 References

Agilent. 2012. *Time Domain Analysis Using a Network Analyzer*. Application Note 1287-12, Agilent Technologies, Santa Clara, California. Available at http://cp.literature.agilent.com/litweb/pdf/5989-5723EN.pdf.

IAEA. 2013. *IAEA Department of Safeguards Long-Term R&D Plan, 2012-2023*. STR-375, International Atomic Energy Agency (IAEA), Vienna, Austria.

Keysight Technologies. 2014. *Keysight Electronic Calibration (ECal) Modules for Vector Network Analyzers - Technical Overview*. Keysight Technologies, Inc. Santa Rose, California. Accessed November 11, 2014. Available at http://literature.cdn.keysight.com/litweb/pdf/5963-3743E.pdf.

LiveWire. 2014. *Live Cable Fault Monitoring*. LiveWire Innovation. South Jordan, Utah. Accessed November 11, 2014. Available at http://livewireinnovation.com/.

Smith LE, P Ramuhalli, DM Sheen, JR Tedeschi, RC Conrad, K Ianakiev, M Browne, J Svoboda, J West and J Sanders. 2014. *Detection of Physical Intrusion in the Cabling of Unattended Safeguards Instruments: Preliminary Requirements and Evaluation Scenarios*. PNNL-23749, Pacific Northwest National Laboratory, Richland, Washington.

Smith P, C Furse and J Gunther. 2005. "Analysis of Spread Spectrum Time Domain Reflectometry for Wire Fault Location." *IEEE Sensors Journal* 5(6):1469-1478.

Wadell BC. 1991. "Transmission Line Handbook" Norwood, MA: Artech House Inc.

# Appendix A

# Preliminary RG71 Cable Testing

# Appendix A

# Preliminary RG71 Cable Testing

To efficiently test devices and taps at different locations, a segmented test cable was developed using three 1.0-meter sections and two 23.5-meter sections to create the 50.0-meter test cable. The test cable will allow for breaks at different locations without requiring a large expensive quantity of 50.0-meter RG71 cables. It is known that the segmentations in the line will produce reflections at the connector interfaces because of impedance mismatches, but these are assumed to be resolvable in the time/spatial domain. The segmented test cable and dimensions are shown in Figure A.1.

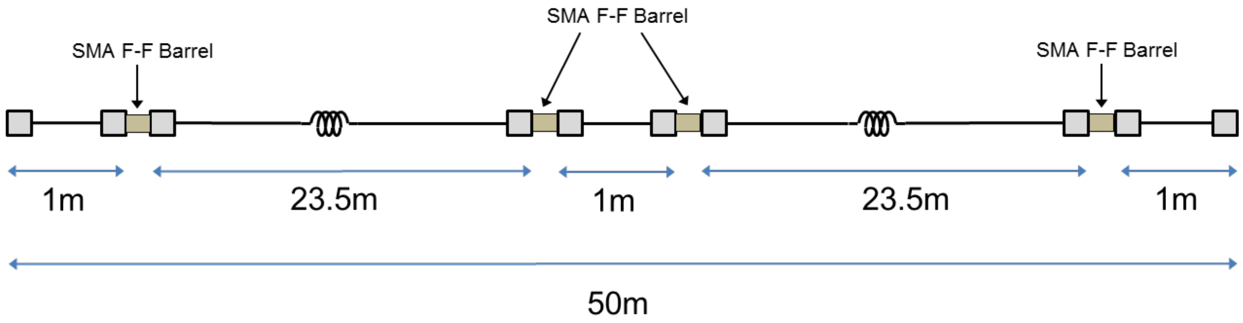

**Figure A.1**. Segmented Cable

The segmented test cable was then connected to the network analyzer to perform a baseline measurement. Note that the cable was fastened down to the table (Figure A.2) to minimize any reflections from cable flexing during measurements.

## A.1 RG71 Segmented Cable TDR Testing and Measurement Results

The baseline measurement for the segmented cable with a 50-ohm load was performed and multiple reflections were observed in the time domain; see Figure A.3. The multiple peak responses are from multiple signal paths traveling from the VNA into the RG71 test cable and reflecting off the sub-miniature Version A (SMA) female barrels–RG71 cable interface.

Figure A.4 shows the multipath reflections happening from the 1.0-m RG71–SMA female barrel interface. The multipath structure creates a complicated response in the spatial domain—changes are still observable but not as dramatic as they would be from a continuous 50-m long cable.

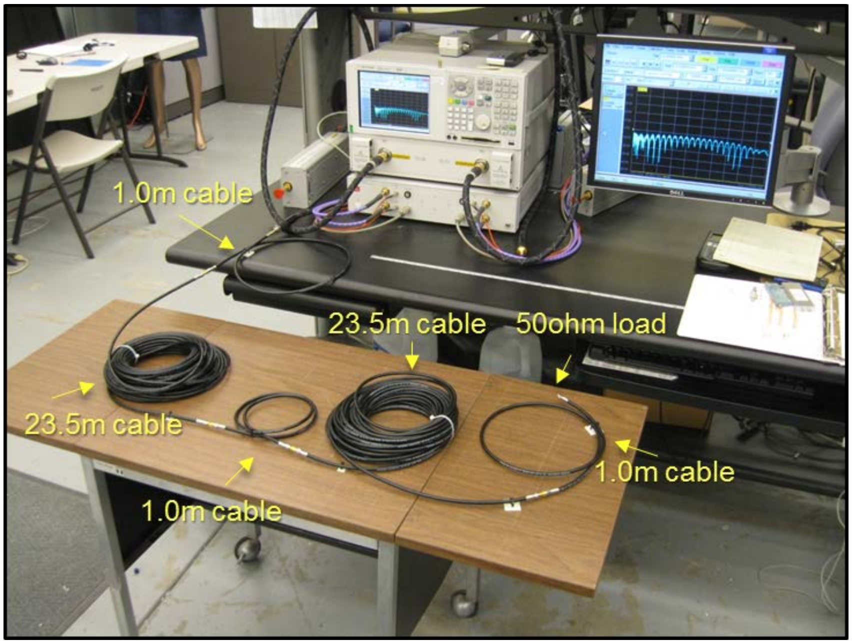

**Figure A.2**. VNA TDR Measurement Configuration

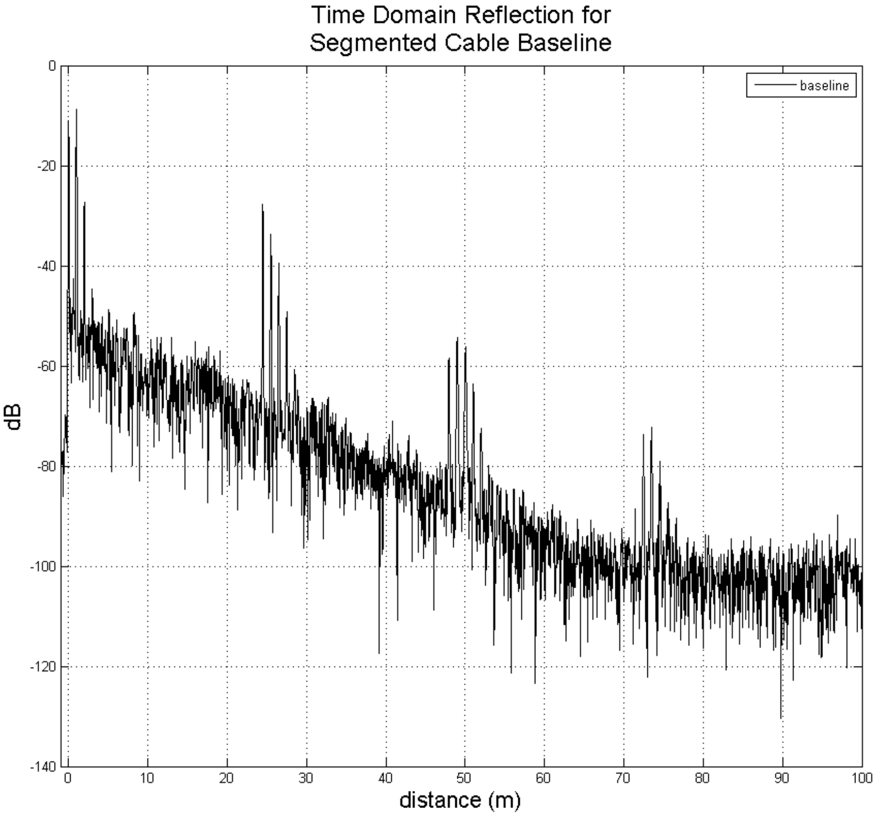

**Figure A.3**. Baseline TDR Measurement for 50-m long Segmented Test Cable

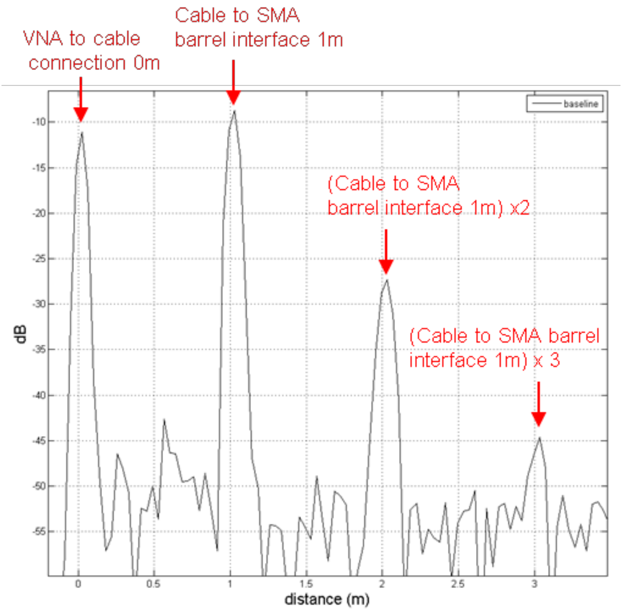

**Figure A.4**. Baseline TDR Measurement Zoomed Span Demonstrating Signal Multipath Response from Reflections off Connector at 1-m Distance

Once the baseline of the test cable was measured, a series of line breaks and signal line tampers were introduced to observe the limitations of the VNA TDR technique. A subset of the measurements that highlights the VNA TDR performance demonstrated the VNA's ability to detect impedance changes at 49 meters; note that 49 m was used as it was not the end of the cable but the farthest interconnection in the segmented test cable. Figure A.5 demonstrates the VNA's TDR measurement capability to detect coaxial line impedance changes at 49 meters.

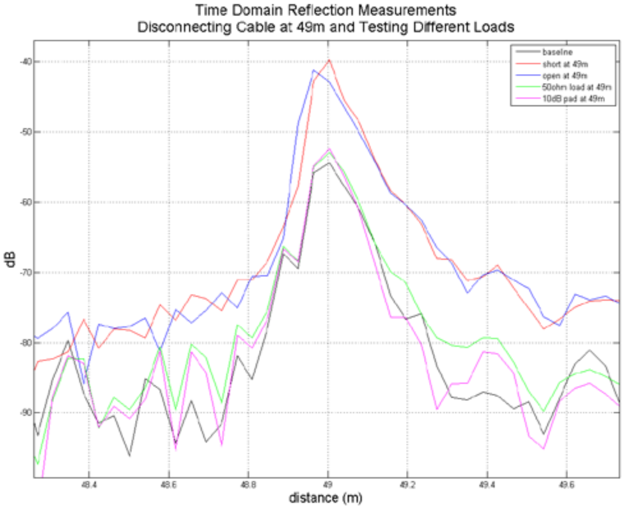

**Figure A.5**. TDR Measurement Results for Coaxial Line Impedance Changes on a 50-m Segmented Cable at 49 m

The results from Figure A.5 demonstrate that the open line and shorted line have a noticeable, ~15 dB increase in reflected signal power compared to the baseline, but the 50-ohm load and 10-dB pad only present a nominal 3-dB increase in reflected signal power when compared to the baseline signal.  This is because the baseline measurement has a large reflection at the measurement location because of the coaxial line transitioning from a 93-ohm cable to a 50-ohm coaxial barrel, which causes a significant reflection.  This is not truly representative of the front-end electronics package for unattended instrumentation scenario, as the coaxial line that will travel from the tamper-proof enclosure to the limited access area will be continuous—any impedance changes from tampering should be compared to the reflections because of the internal structure of the coaxial cable, not any interconnection interfaces.  If this were the case, the scenario displayed in Figure A.5 would compare the 50-ohm termination and 10-dB pad to the cable structure, which is on the order of −80 dB, so it would have a change in reflected power of ~25 dB instead of 3 dB.

With this understanding gained, the segmented cable testing was put on hold with the new focus being tamper measurements of continuous RG174 cable.  RG174 is a 50-ohm coaxial cable and will impedance match cable tamper devices under test as it is the industry standard for nearly all SMA connectorized microwave components to be matched to 50 ohms.

www.pnnl.gov

Pacific Northwest
NATIONAL LABORATORY

*Proudly Operated by* **Battelle** *Since 1965*

U.S. DEPARTMENT OF
ENERGY

902 Battelle Boulevard
P.O. Box 999
Richland, WA 99352
**1-888-375-PNNL** (7665)